Acta Geotechnica (2011) 6:41–49
DOI 10.1007/s11440-011-0134-7

RESEARCH PAPER

Structural optimization in geotechnical engineering: basics and application

T. Pucker · J. Grabe

Received: 20 August 2010 / Accepted: 14 February 2011 / Published online: 9 March 2011

Abstract Structural optimization methods are used for a wide range of engineering problems. In geotechnical engineering however, only limited experience exists with these methods. The difficulties in applying such methods to geotechnical problems are discussed in this paper, and the adaption of the commonly known SIMP-method to geotechnical problems is introduced for a special case. An application example is used to present the potential of topology optimization methods, and the application to geotechnical engineering is evaluated.

Keywords Geotechnic · Hypoplasticity · Optimization · Topology

1 Introduction

Optimization of structural topology, shape and material is state-of-the-art in a wide area of engineering applications. Methods of topology optimization are especially used to reduce weight, costs and material in the automotive and aircraft industries. The methods of structural optimization allow an automatic development of the optimal design of construction elements. Depending on the particular application, it is possible to generate an optimized structure from an unshaped block element. The coupling of structural optimization methods with numerical simulation software, such as the Finite Element Method, allows the simulation and estimation of almost any imaginable geometry. In structural engineering, the development and application of such optimization methods have only recently been initiated. This due to the differences between structural and mechanical engineering. Mass productions are aimed at mechanical engineering, where a small reduction in costs can enable large savings. In structural engineering, however, the product typically is a individual one-off design. The application of optimization methods in geotechnics is uncommon to date. Until now, optimization methods are used in geotechnics e.g. to determine slope stability (Baker and Gaber [2]). Another application of optimization is the inverse soil parameter determination (Zhang et al. [21] and Meier et al. [11]). An application of optimization af a geotechnical design process can be found in Kinzler [8]. The potential of these methods is shown by the results of the application in other engineering areas. In geotechnical engineering, these methods are able to support the engineer in achieving economic designs, even if the problem is very difficult and complex. In the strategies of optimization in automotive and aircraft industries, merely the structure of homogeneous materials is optimized. This contrasts with geotechnical engineering, where two different materials, structure and soil, have to be considered. In this paper, the development and application of structural optimization methods in geotechnics are demonstrated. Several methods to solve strutural optimization problems have been developed. A review of the most common formulations can be found by Arora and Wang [1]. The SIMP-Method of Sigmund [17], a combined method of topology and shape optimization, is described and used. This method is very robust and the link-up to a finite element programm can be realised simply.

T. Pucker (✉) · J. Grabe
Institute of Geotechnical Engineering and Construction Management, Hamburg University of Technology, Harburger Schloßstr. 20, 21079 Hamburg, Germany
e-mail: tim.pucker@tu-harburg.de

J. Grabe
e-mail: grabe@tu-harburg.de

2 Terminology

Structural optimization is divided in topology optimization, shape optimization and dimension optimization. Most of the structural optimization methods are developed especially for one of these three groups.

Topology stems from the greek terms lógos (teaching) and tópos (location). It is an area of mathematics that describes structures geometrically. The topology is the main design of a structure. The terminology 'topology' is illustrated with a geotechnical example in Fig. 1. Figure 1a shows the actual design problem, a surface jump has to be stabilized. Three different solutions are shown in Fig. 1a,b,c. The solutions differ in their topology.

Once a topology is chosen, its shape can be improved. It is not possible to change the topology during a *shape optimization*. The topology in Fig. 1d is chosen for this example. Figure 2 shows three alternatives to achieve the optimization objective. In this case, the maximum wall deflection is a possible optimization object. To achieve an economic design for the chosen topology, it is reasonable to vary the anchor position (Fig. 2b), the anchor inclination (Fig. 2c) and the anchor length (Fig. 2d).

Dimension optimization defines the profile properties of the individual structural elements. Neither the topology nor the shape can be changed by the dimension optimization. This group of structural optimization is the most widely applied method in structural engineering, because most analysis software provides this option. In our example, the shape optimization in Fig. 2 results in the the optimal shape shown in Fig. 3. In this case, the dimension optimization defines for instance the wall profile, the anchor profile and the dimensions of the grouted anchor.

3 SIMP-method

The SIMP-method (Solid Isotropic Material with Penalization) is a very popular and efficient method for topology optimization (Sigmund [17]). This method is based on the idea that the required material is already uniformly placed in the design domain Ω. The optimal subset that represents the optimal topology of this domain is called Ω^{mat}. The SIMP-Method seeks iterativly the optimal subset. The design domain Ω is discretized with finite elements. The material properties are constant in each of these elements und depend on the relative density ρ. The relative density varies over the design domain. The material is concentrated at highly loaded locations and less concentrated in areas of low stress. The relative density should be either 1 or 0 at every point a in the design domain Ω after the optimization:

$$\rho(a) = \begin{cases} 0 \rightarrow \text{no material} \\ 1 \rightarrow \text{material} \end{cases} \tag{1}$$

The goal of the optimization method is to minimize the compliance of the structure in the design domain Ω. Thus, the stiffness is maximized.

The compliance of a structure can be expressed using the internal energy of the system. The internal energy c of an elastic material is defined by:

$$c(\boldsymbol{x}) = \mathbf{U}^T\mathbf{K}\mathbf{U} \tag{2}$$

where $\mathbf{U}$ is the global deformation tensor, $\mathbf{K}$ the global system stiffness matrix and $\boldsymbol{x}$ the tensor of the design parameters. The design parameters x_i of the tensor $\mathbf{x}$ are distributed over the design domain. These are variable parameters that have to be chosen for the specific case, i.e. the elastic modulus E, the Poisson's ratio ν, the friction angle φ, etc. This optimization method considers two different constraints. The first constraint is in this case expressed with the equilibrium:

$$\mathbf{K}\mathbf{U} = \mathbf{F} \tag{3}$$

where $\mathbf{F}$ is the tensor of the external forces.

The second constraint demands that the volume of the design structure decreases or remains equal to the volume V_0 at the beginning of the optimization process. The SIMP-Methods assumes constant volume:

$$\int_{\Omega^{mat}} 1 d\Omega = V_0 \tag{4}$$

The design parameters x_e are limited by an upper and a lower bound, such that the material properties correspond

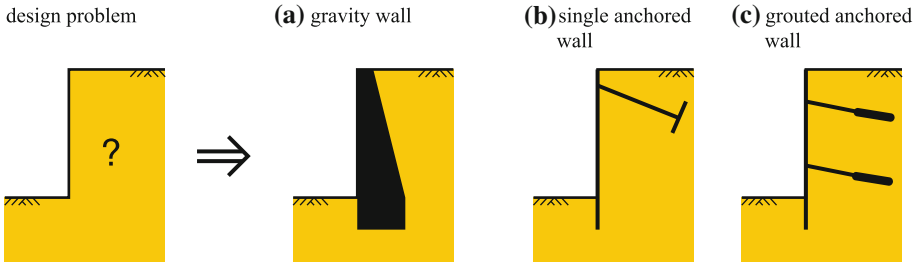

Fig. 1 Topology optimization for a design problem, **a** gravity wall, **b** single anchored wall, **c** double anchored wall with grouted anchor

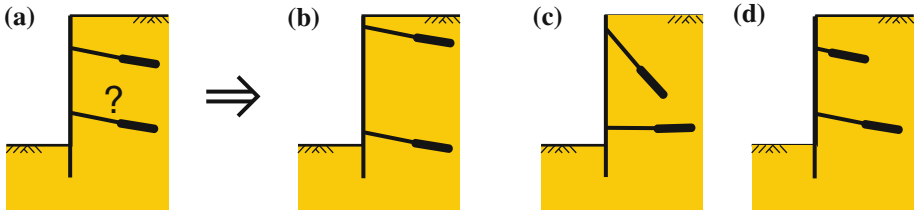

Fig. 2 Shape optimization: **a** chosen topology, **b** variation 1: anchor position, **c** variation 2: anchor inclination, **d** variation 3: anchor length

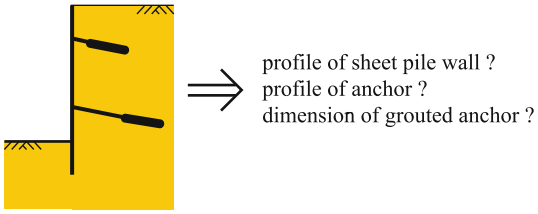

Fig. 3 Dimension optimization

to the physically possible range. The optimization task for minimal compliance design can be cast as:

$$\left.\begin{array}{ll} \text{min:} & c(\boldsymbol{x}) = \mathbf{U}^T\mathbf{K}\mathbf{U} = \sum_e^N (\rho_e)^p u_e^T K_e u_e \\ \text{subject to :} & \mathbf{K}\mathbf{U} = \mathbf{F} \\ & V_\delta = V_0 \cdot \delta \\ & 0 < \rho_{min} \leq x_e \leq 1 \end{array}\right\} \quad (5)$$

where u_e is the element displacement tensor, K_e the element elasticity matrix and ρ_e the relative density of the element. The internal energy in the design domain Ω cannot be minimized, because the external energy has to equal the internal energy for the equilibrium in the Finite Element Method. Therefore, the internal energy is multipled with the relative density for each element. To reach the minimum compliance design, the sum of the internal energy in elements with a high relative density is minimized. $c(x)$ is also called compliance, so it is a minimal compliance optimization. A lower bound of $\rho_{min} > 0$ for the relative density is established to avoid numerical singularities. The material change-over is controlled by a penalty term p, which is commonly chosen to $p = 3$ [4]. In the element e, the Young's modulus E changes from E_1 to E_2 depending on the virtual density ρ_e during the optimization:

$$E_2 = E_1 \cdot (\rho_e)^p \quad (6)$$

This equation is used to demonstrate the influence of the penalty term p, see Fig. 4. If the penaltiy term is too small, the material change-over cannot finish completely during the optimization process. Hence, in such cases, the results cannot be interpreted because the material surface cannot be identified. Bendsøe [4] proposed to select $p \geq 3$ in two-dimensional and $p \geq 2$ in three-dimensional space. After the application of the SIMP-Method in Sect. 5, the result (Fig. 8d) is checked regarding the material change-over. It can be seen that the material change-over finished nearly

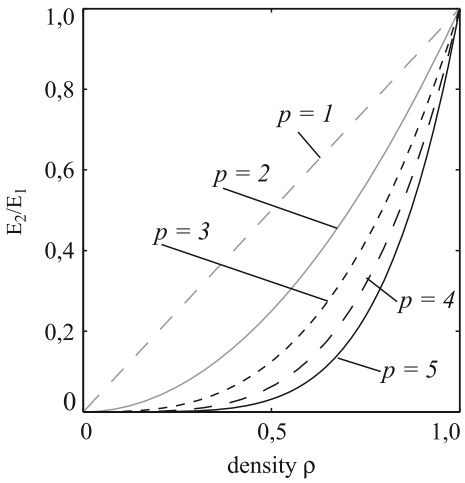

Fig. 4 Change-over of the Young's modulus E of two different materials depending on different values of the penalty term p

completely in all elements, so the choice of the penalty term $p = 3$ for this application is well chosen.

The volume V_δ corresponds with the volume V_0 of the design domain where δ is the volume fraction. To solve the optimization task, the method of optimal criteria is used as predefined by Bendsøe [4]:

$$\rho_e^{new} = \begin{cases} \max(\rho_{\min}, \rho_e - m) \\ \quad \text{if } \rho_e B_e^\eta \leq \max(\rho_{\min}, \rho_e - m) \\ \rho_e B_e^\eta \\ \quad \text{if } \max(\rho_{\min}, \rho_e - m) < \rho_e B_e^\eta < \min(1, \rho_e + m) \\ \min(1, \rho_e + m) \\ \quad \text{if } \min(1, \rho_e + m) \leq \rho_e B_e^\eta \end{cases} \quad (7)$$

A positive move-limit m and a numerical damping coefficient $\eta = 0.50$ are introduced, see Bendsøe [4]. The values for m and η are chosen by experiment to reach a stable convergence of the iteration scheme. The sensitivity of the objective function is expressed as

$$\frac{\partial c}{\partial \rho_e} = -p(\rho_e)^{p-1} u_e^T K_e u_e \quad (8)$$

and B_e is defined through the Lagrangian multiplier λ:

$$B_e = \frac{-\partial c/\partial \rho_e}{\lambda \partial V/\partial \rho_e} \quad (9)$$

Sigmund [17] uses a filter to ensure a unique solution of the optimization task. The filter modifies the element sensitivity, so the solution does not depend on the discretization level. Further detail can be found in Sigmund [15, 16].

4 Adaptation of the SIMP-method to geotechnical engineering

The main assumption of the SIMP-method is the homogeneity of the material in the structure. The elements in the design domain with no material are disabled by assigning very soft material properties. The homogeneous material is modelled generally with linear elastic material behaviour. In geotechnics, at least two different material types, the soil and the structure, have to be considered. The material behaviour of soils is highly nonlinear and cannot be reproduced adequately with a linear elastic or a linear elastic - ideal plastic constitutive model.

4.1 SIMP-method adaption requirements

The adaption of the SIMP-method in geotechnics requires primarily the consideration of two different types of materials. Therefore, the volume V_0 (see Eq. 4) is defined as the volume of the structural parts only. In the particular case of linear elastic material behaviour of both materials, the material parameters of soft material relates to the virtual density $\rho = 0$. The virtual density of $\rho = 1$ relates to the stiff material. The material parameters between the limits of the relative density, $0 < \rho < 1$, are labelled as change-over material. The mathematic function to describe the change-over process is expressed with the given example of Young's modulus change-over:

$$E = E_0 + (E_1 - E_0) \cdot (\rho_e)^p \tag{10}$$

E is the Young's modulus in a particular element, E_0 of the soft material and E_1 of the stiff material. The stiffness of the change-over material has to increase with increasing virtual density ρ to minimzie the compliance. Decreasing compliance strictly requires increasing material stiffness. If the stiffness of the change-over material does not increase continuously related with the virtual density, it is possible to reach a local minimum of the objective function. In this case, the material change-over cannot be completed.

4.2 Material change-over in geotechnics

As stated above, a sophisticated constitutive model is required to reproduce the salient material behaviour. In the present paper, the hypoplastic constitutive model of von Wolffersdorff [19] with the extension of intergranular strain by Niemunis and Herle [12] is used. Hypoplastic model was originally developed for cohesionless materials. Recently, the model was extended to include cohesive soils (Huang et al. [7], Weifner and Kolymbas [20], Mašín and Herle [10], Bauer [3]). Numerical investigation of boundary value problems using hypoplastic constitutive models was reported recently by Henke and Grabe [6], Salciarini and Tamagnini [14], Tejchman and Górski [18]. The identification of parameters in the hypoplastic model was discussed by Rondón et al. [13], Guo [5] for a large number of soil types. The constitutive model is able to reproduce the nonlinear and anelastic behaviour of soils close to reality. Specific properties of soils are considered, including dilatancy, different stiffnesses for loading and unloading paths, barotropy and pyknotropy. The extension of intergranular strain allows the simulation of effects such as accumulation of deformation and hysteretical behaviour under cyclic loading to be modelled appropriately. The constitutive model is expressed in a rate-dependent form defined by the tensor function:

$$\overset{\circ}{\mathbf{T}} = \mathcal{M}(\mathbf{T}, e, \boldsymbol{\delta}) : \mathbf{D} \tag{11}$$

In this equation, $\overset{\circ}{\mathbf{T}}$ is the objective stress rate, $\mathbf{D}$ the strain rate and $\mathcal{M}$ a fourth order tensor, which depends on the actual Cauchy stress $\mathbf{T}$, the void ratio e and the intergranular strain $\boldsymbol{\delta}$. The input of 14 material parameters is necessary to use this constitutive model (Table 1).

In contrast to linear elasticity, the material change-over from a soft to a stiff material, coupled with a linear interpolation of the virtual density, is limited to rare cases. The material change-over as shown in Eq. 10 frequently leads to a temporary material loosening such that a local

Table 1 Material parameters for the hypoplastic constitutive model with intergranular strain

Parameter	Description
φ_c	Critical state friction angle
h_s	Granular hardness
n	Exponent
e_{d0}	Minimal void ratio
e_{i0}	Critical void ratio
e_{c0}	Maximal void ratio
α	Exponent
β	Exponent
R	Maximum value of intergranular strain
m_R	Stiffness ratio at a change of direction of 180°
m_T	Stiffness ratio at a change of direction of 90°
β_R	Exponent
χ	Exponent
e_0	Void ratio at a stress state of $\sigma = 0$ kN/m^2

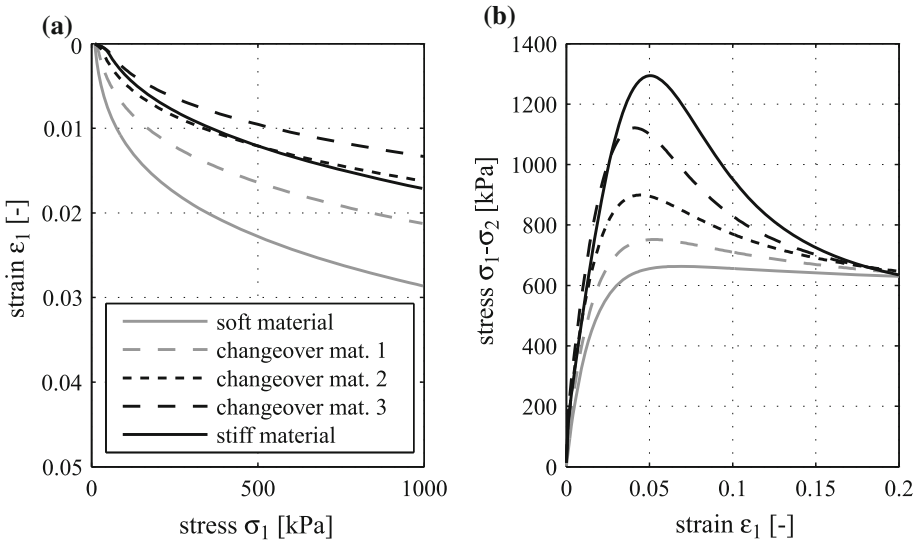

Fig. 5 Material behaviour of a stiff, a soft material and the according change-over materials, **a** oedometric test, **b** triaxial test

minimum of the objective function can be reached. Due to this effect, the change-over of every single material parameter has to be determined individually. Figure 5 shows the results of an oedometric and a triaxial test. The soft material, the stiff material and also three steps of the material change-over are tested. The material parameters of the soft and the stiff material are listed in Table 2. The material change-over is interpolated linearly in this example. The steps of the change-over are plotted for the densities $\rho = 0.25; 0.50; 0.75$. The oedometric test starts at a stress level of 10 kN/m^2 and is loaded to 1,000 kN/m^2. The unloading and reloading paths are not shown in this Figure. The triaxial test is performed with a cell pressure of $\sigma_2 = 200$ kN/m^2, and the sample is loaded until a maximal strain of $\varepsilon_1 = 20\%$ is reached. Figure 5b shows the increasing resistance $q_{max} = \max(\sigma_1 - \sigma_2)$ of the material over the change-over steps. The stiffness of the material, see Fig. 5a, increases over the first change-over steps. After the third change-over step, the stiffness exceeds to the stiffness of the stiff material. Thus, some of the change-over materials have better properties than the stiff structure material. The SIMP-method minimizes the compliance by changing the material or its properties and stiffens the behaviour. Hence, the material change-over cannot finish completely and remains in step three.

Figure 6a shows a rare case. All material parameters can be linearly interpolated depending on the virtual density. The resistance q_{max} increases with the relative density, see Fig. 6b. The stiffness increases over the material change-over in the oedometric test and reaches its maximum stiffness value with the stiff material (Fig. 6a). The material parameters for both materials can be linearly interpolated and are applicable for the SIMP-method and Eq. 10.

Table 2 Hypoplastic material parameters for the examples of material change-over

Parameter	φ_c	h_s [MPa]	n	e_{d0}	e_{i0}	e_{c0}	α	β
Nonlinear material change-over								
Soft material	36	3.2e7	0.18	0.53	0.73	0.80	0.08	1.80
Stiff material	33	1.5e6	0.28	0.55	0.95	1.05	0.25	1.05
Linear material change-over								
Soft material	30	5.8e6	0.28	0.53	0.84	1.00	0.13	1.05
Stiff material	45	1.5e6	0.28	0.55	0.95	1.05	0.50	3.05

Parameter	m_R	m_T	R	β_R	χ	e_0
Nonlinear material change-over						
Soft material	2.0	1.0	1e-4	0.5	6.0	0.65
Stiff material	2.0	1.0	1e-4	0.5	6.0	0.65
Linear material change-over						
Soft material	2.0	5.0	1e-4	0.5	6.0	0.65
Stiff material	2.0	5.0	1e-4	0.5	6.0	0.65

4.3 Implementation

The SIMP-method is coupled here with the commercial finite element method program Abaqus/Standard, Version 6.8. The method is implemented with an external stand-alone program routine. The routine calculates the distribution of the relative density and executes the finite element calculation. The compliance is evaluated after each successful calculation, and a new distribution of the relative density is defined. In this way the system is optimized iteratively.

Abaqus/Standard offers the possibility to use material behaviour depending on the actual temperature. The

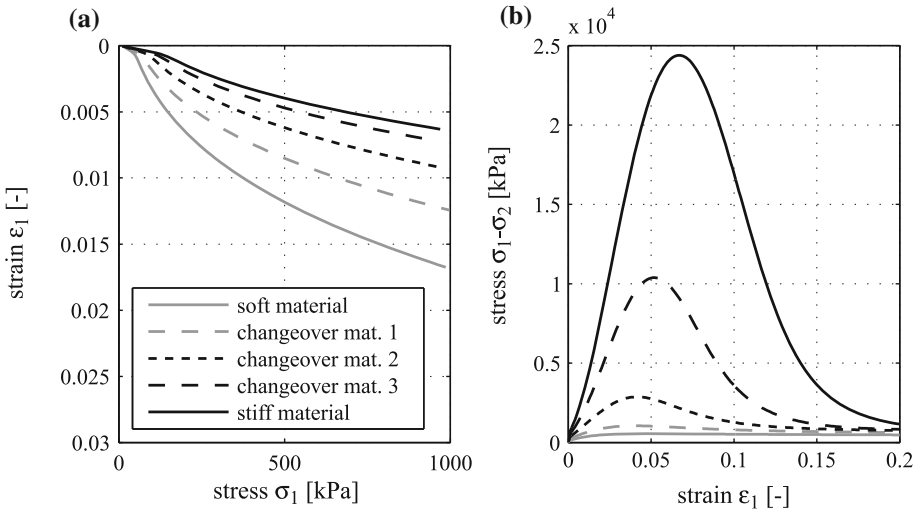

Fig. 6 Special case: material behaviour of a stiff, a soft material and the according change-over materials, **a** oedometric test, **b** triaxial test

material parameters can be defined regarding different temperature states. This option is used to obtain the correlation between the material parameters and the relative density. The distribution of the relative density is set equal to a virtual temperature state $T(x)$ in the finite element calculation. The temperature can reach values between $0\ \mathrm{K} < T(x) < 1\ \mathrm{K}$. The material properties of elements with a temperature of $T = 0$ K relate to the soft material and elements with $T = 1$ K relate to the stiff material. The hypoplastic constitutive model is implemented in Abaqus via a user subroutine, which has to be extended for a temperature-depending soil parameter definition. The material change-over occurs according to Eq. 10.

5 Application

The estimated settlement and inclination of a structure affect mainly its usability and thus usually describe the main boundary conditions in geotechnics. In this application, the potential of the supposed topology optimization method is demonstrated using the example of a simple strip foundation. An optimized foundation structure topology has to be developed under an already existing foundation. The objective function is given in Eq. 5. A resulted settlement reduction can be shown with this simple example. The soil and all structural parts are discretized with 4-node volume elements with reduced integration and linear approach. The contact between the existing structural parts and the soil is modelled as hard contact in the normal direction and frictionless in the tangential direction. The contact surface between soil and developing foundation cannot be identified exactly with the optimization process; therefore, no contact formulation is considered. It is assumed that the foundation structure does not move relatively to the soil.

The behaviour of the already existing foundation is simulated with a linear elastic constitutive model. The Young's modulus is $E = 3.2 \cdot 10^7$ kN/m^2 and the Poisson's ratio $\nu = 0.2$. Both soil and new foundation structure are simulated with the hypoplastic constitutive model of von Wolffersdorff [19] with the extension of intergranular strain of Niemunis and Herle [12]. The material parameters for this model are listed in Table 2. Parameters of the linear material change-over for the soft material correspond to the parameters of the soil and the stiff material correspond to the parameters of the foundation structure.

The initially existing strip foundation is 2 m wide and 1 m deep (Fig. 7) and loaded with a force $P = 500$ kN.

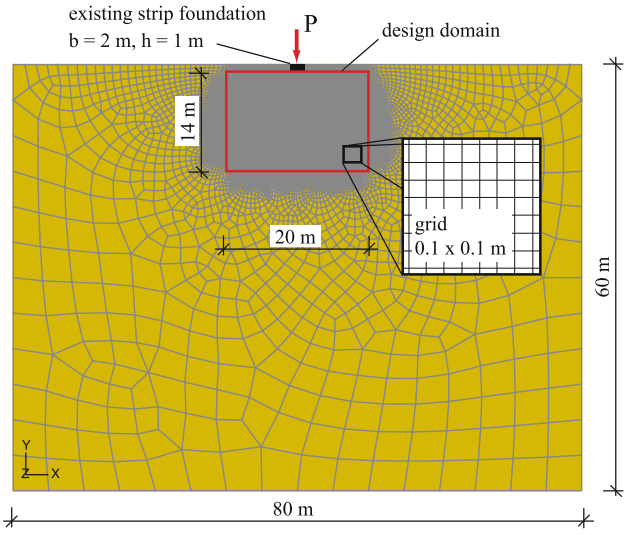

Fig. 7 Discretization of the FE-model of a strip foundation with a width of 2 m and a depth of 1 m, loaded with 500 kN by the point load P

Symmetrical properties of the system are not utilized, so the optimized foundation structure can be checked for plausibility. Three different optimization runs are calculated with different material volumes: 2, 5 and 10% of the design domain Ω. The design domain of the foundation structure ist placed directly unter the existing foundation and has dimensions of 20 × 14 m (Fig. 7). The distribution of the virtual density shall be represented detailed enough, so the design domain is discretized with elements of the size 0.1 × 0.1 m. Due to preexamination, the penalty term p is set to $p = 3$ and the radius filter to $r_{min} = 1.5$.

Figure 8 shows the different evolution states of the foundation structure with a material volume of 2% of the design domain. In the first step (Fig. 8a), the material is compacted under the existing strip foundation and is placed in the pressure bulb. The evolution state after 15 iterations is shown in Fig. 8b. The material compacts directly under the strip foundation and develops a vertical structure under the footing edges. The theoretical solution of an inflexible foundations on an elastic half-space leads to stress peaks under the foundation edges. In this area, the optimization algorithm increases the relative material density. Figure 8c shows the topology of the foundation structure after 50 iteration. The material distribution changed marginally compared with the evolution state after 15 iterations. The material compaction under the strip foundation edges is clearly shown after 500 iterations in Fig. 8d. Material is placed under the footing edges mainly in the vertical direction. In this way the stress peaks are transferred to deeper layers.

Figure 9 shows the settlements of the soil. The origin design without the optimized foundation structure (Fig. 9a) settles about 4.4 cm. Figure 9b shows the displacement of the optimized foundation structure. The achieved settlements of about 2.4 cm under the strip foundation relates to 48% of the primary displacement.

A correlation between the used material volume and the minimal possible settlement can be estimated with the different optimization runs. This correlation is plotted in Fig. 10. Due to the assumption, that this optimization method reaches a global optimum, the points on the graph in Fig. 10 fit the EDGEWORTH-PARETO-set of an optimization with the criteria of minimal settlement and minimal volume, see also [9]. This set is characterized by the fact that no criteria can be improved without compromising another. In this example, the settlement in one point cannot be improved without compromising the volume in that point. Every point of the EDGEWORTH-PARETO-set is

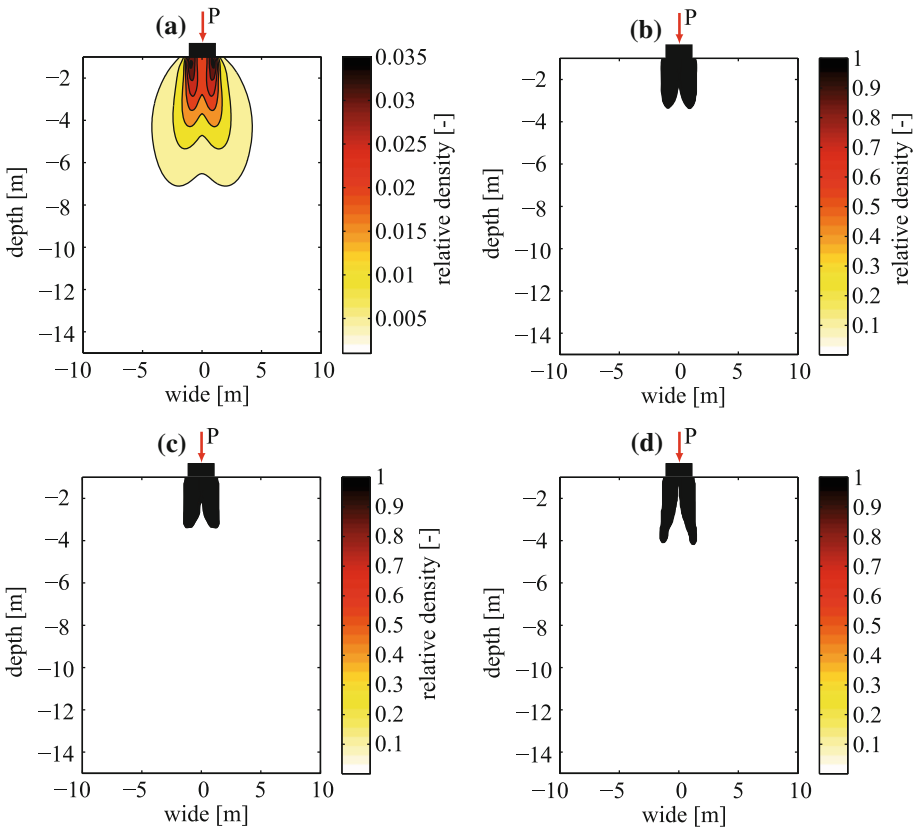

Fig. 8 Evolution states of the foundation structure with a material volume of 2% of the design domain; evolution state after 1 (**a**), 15 (**b**), 50 (**c**) and 500 (**d**) iterations

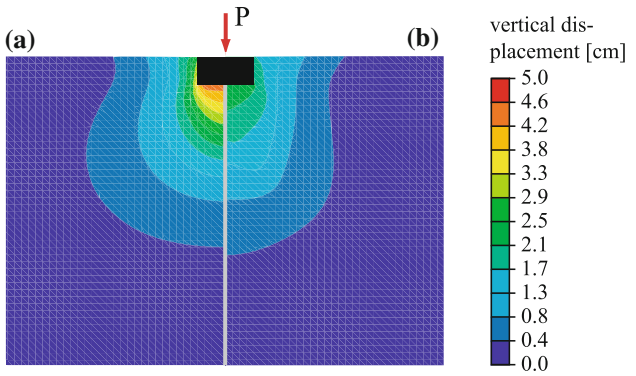

Fig. 9 Vertical displacements before **a** and after **b** the optimization

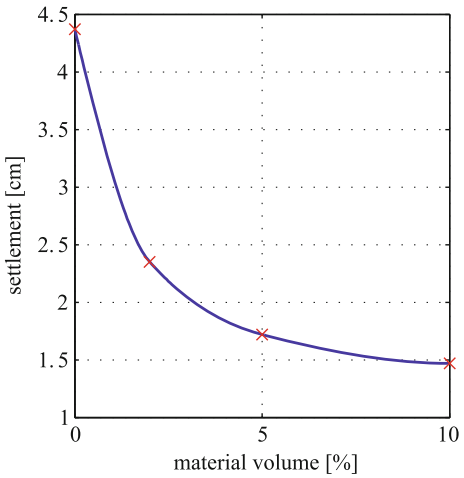

Fig. 10 Minimal settlement of the strip foundation depending on the used material volume

at the optimum. For a given settlement of this foundation, the minimum volume of the foundation can be obtained from Fig. 10.

6 Practical realisation

Structurally optimized design puts high demands on current methods of construction. The optimization algorithms develop a geometric shape of a structure without consideration of its practicability. The accurate transcription of a topology-optimized structure may therefore imply enormous costs. It may even be impossible to construct such a structure. This leads to the conclusion that the construction method for the estimated result and the relevant materials have to be chosen a priori. The jet grouting method is a suitable example. This method forces a cement emulsion into the soil. The emulsion hardens and cements the soil grains. A compact jet grouting structure develops. This method allows to realize almost every optional geometry. Another way to use topology-optimized designs ist to

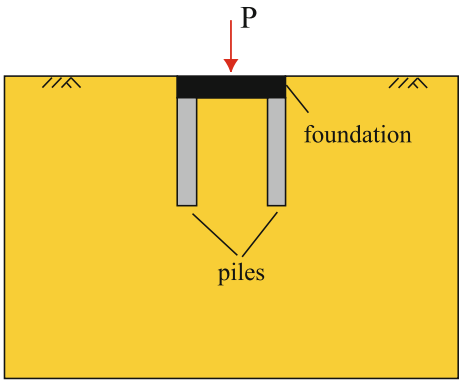

Fig. 11 Example: Interpretation of the topology-optimized design

interpret and to adjust the design regarding possible construction methods. An example is given in Fig. 11. In this way, the structural optimization is not used to obtain the globally optimal structure, but it is used to better understand the flow of forces in complex design tasks and to elaborate a practicable design. However, this strategy does not fully utilize the potential of the optimization method.

7 Conclusion

The applicability of structural optimization methods, especially of the topology optimization in geotechnical engineering, can be demonstrated in this paper. The optimized topology of the application example can be explained with classical theory of soil mechanics. The realization of such topologies is partially possible with the current construction methods, such as the jet grouting. Further investigation is required for the interpretation of optimized structures regarding the application to other construction methods due to the costs of complex topologies. Nevertheless, the potential of the structural optimization methods has been demonstrated. These methods provide significant opportunities in the design process of geotechnical engineering.

References

1. Arora JS, Wang Q (2005) Review of formulations for structural and mechanical system optimization. Struct Multidiscip Optim 30:251–272
2. Baker R, Garber M (1977) Variational approach to slope stability. Proceedings of the ninth international conference on soil mechanics and foundation engineering
3. Bauer E (2009) Hypoplastic modelling of moisture-sensitive weathered rockfill materials. Acta Geotech 4:261–272
4. Bendsøe MP (1995) Optimization of structural topology, shape and material. Springer, Berlin

5. Guo PJ (2010) Effect of density and compressibility on K0 of cohesionless soils. Acta Geotech 5:225–238
6. Henke S, Grabe J (2008) Numerical investigation of soil plugging inside open-ended piles with respect to the installation method. Acta Geotech 3:215–223
7. Huang WX, Wu W, Sun DA, Sloan S (2006) A simple hypoplastic model for normally consolidated clay. Acta Geotech 1:15–27
8. Kinzler S, König F, Grabe J (2007) Entwurf einer Pfahlgründung unter Anwendung der Mehrkriterienoptimierung. Bauingenieur 82:267–379
9. Krishnan S (2010) A 199-line Matlab code for Pareto-optimal tracing in topology optimization. Struct Multidiscip Optim 42:665–679
10. Mašín D, Herle I (2007) Improvement of a hypoplastic model to predict clay behaviour under undrained conditions. Acta Geotech 2:261–268
11. Meier J, Schaedler W, Botgatti L, Schanz T (2008) Inverse paramter identification technique using PSO algorithm applied to geotechnical modeling. J Artif Evol Appl
12. Niemunis A, Herle I (1998) Hypoplastic model for cohesionless soils with elastic strain range. Mech Frict Cohesive Mater 2:279–299
13. Rondón HA, Wichtmann T, Triantafyllidis Th, Lizcano A (2007) Hypoplastic material constants for a well-graded granular material for base and subbase layers of flexible pavements. Acta Geotech 2:113–126
14. Salciarini D, Tamagnini C (2009) A hypoplastic macroelement model for shallow foundations under monotonic and cyclic loads. Acta Geotech 4:163–176
15. Sigmund O (1994) Design of material structures using topology optimization, Ph.D. Thesis, Department of Solid Mechanics, Technical University of Denmark
16. Sigmund O (1997) On the design of compliant mechanisms using topology optimization. Mech Struct Mach
17. Sigmund O (2001) A 99 line topology optimization code written in Matlab. Struct Multidiscip Optim 21:120–127
18. Tejchman J, Górski J (2010) Finite element study of patterns of shear zones in granular bodies during plane strain compression. Acta Geotech 5:95–112
19. von Wolffersdorff P-A (1996) A hypoplastic relation for granular materials with a predefined limit state surface. Mech Frict Cohesive Mater 1:251–271
20. Weifner T, Kolymbas D (2007) A hypoplastic model for clay and sand. Acta Geotech 2:103–112
21. Zhang Y, Gallipoli G, Augarde CE (2009) Simulation-based calibration of geotechnical parameters using parallel hybrid moving boundary particle swarm optimization. Comput Geotech 36:604–615